Supplementary 1

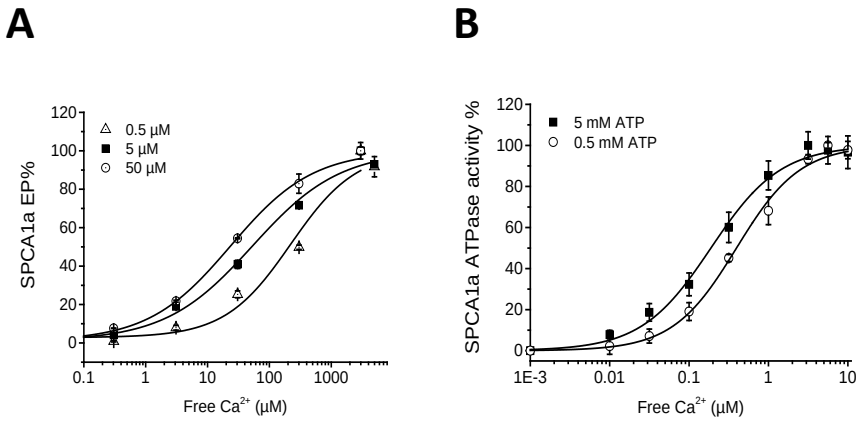

Supplementary 2

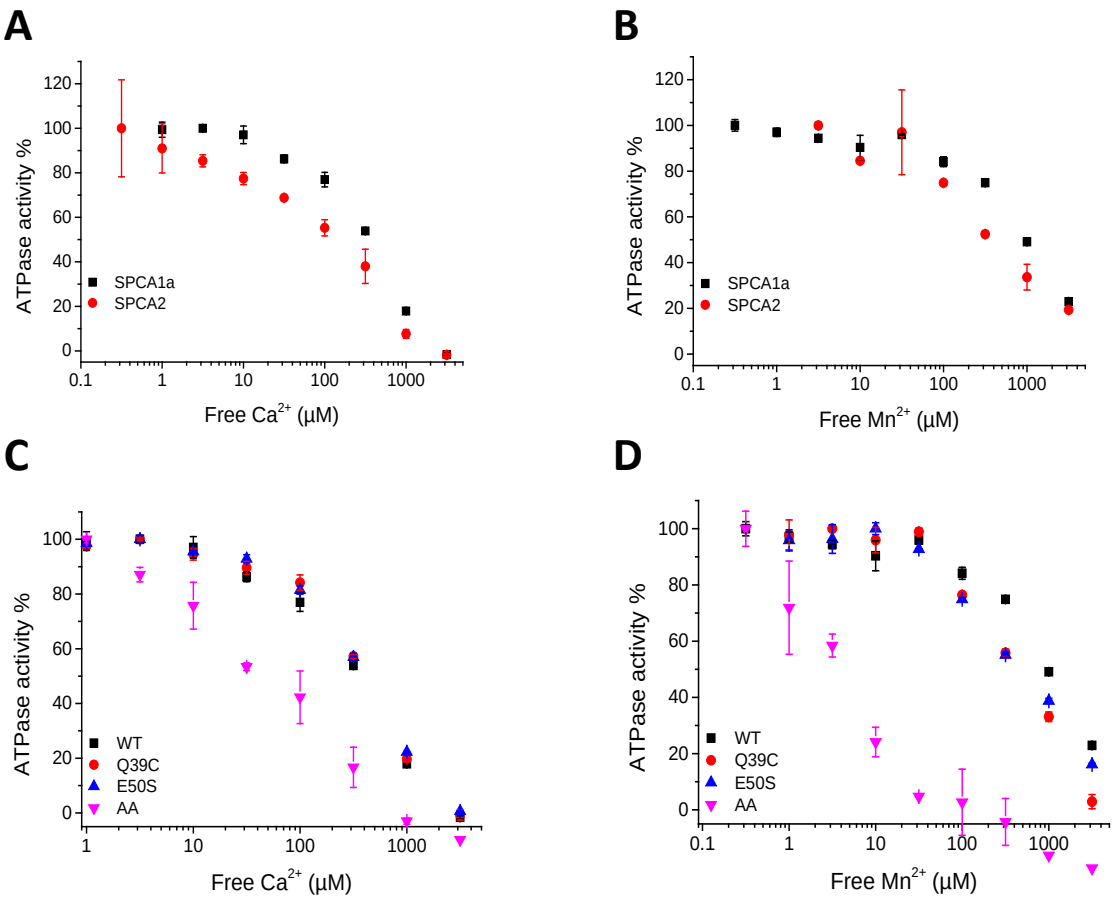

Supplementary 3

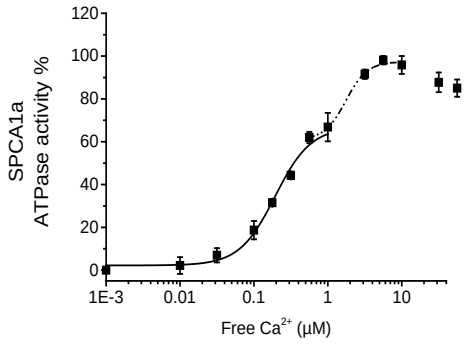

Supplementary 4

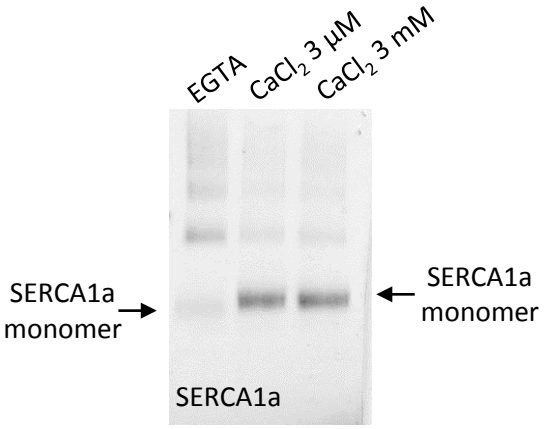

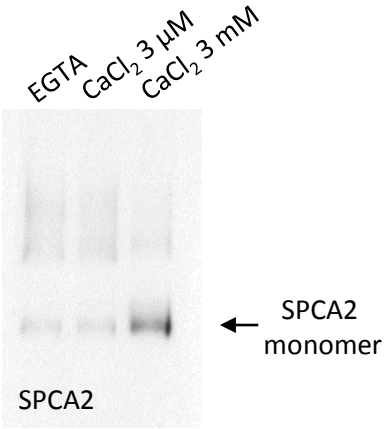

Supplementary 5

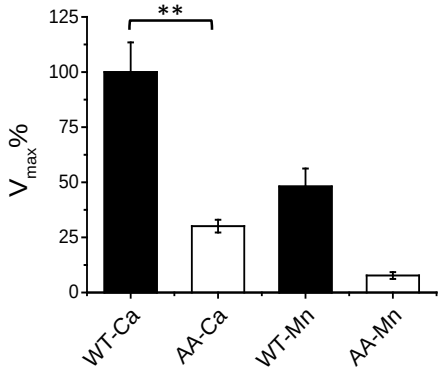

Supplementary 6

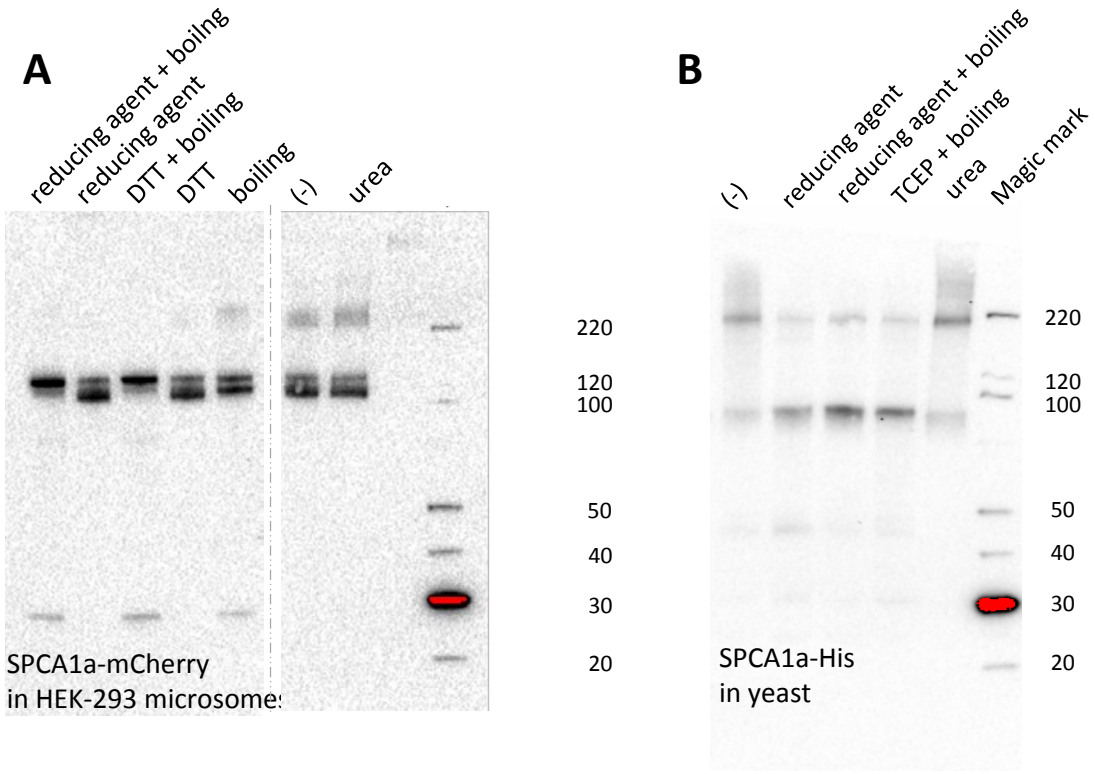

Title: An N-terminal Ca^{2+} binding motif regulates the secretory pathway Ca^{2+}/Mn^{2+}-ATPase SPCA1

Authors: Jialin Chen, Susanne Smaardijk, Charles-Alexandre Mattelaer, Filip Pamuła, Ilse Vandecaetsbeek, Jo Vanoevelen, Frank Wuytack, Eveline Lescrinier, Jan Eggermont, Peter Vangheluwe

Supplementary figure legends

Suppl. Fig. 1. Changes in ATP concentration affect the apparent Ca^{2+} affinity of SPCA1a
A. Ca^{2+} dependent phospho-intermediate levels at varying total ATP concentrations were quantified by radio-activity measurements. B. Ca^{2+} dependency of the ATPase activity at varying ATP concentrations (N = 4). The ATP concentrations was kept constant by a regenerating enzyme system. In both the auto-phosphorylation assay (A) and the enzyme-coupled ATPase assay (B), the apparent Ca^{2+} affinity of SPCA1a decreases when the ATP concentration is reduced. Increase of ATP concentration in the auto-phosphorylation assay increases the apparent Ca^{2+} affinity.

Suppl. Fig. 2. Back-inhibition of the ATPase activities at high Ca^{2+} or Mn^{2+} concentrations
ATPase activities were measured for wild-type SPCA1a and SPCA2 at Ca^{2+} (A) or Mn^{2+} (B) concentrations above 10 µM. This resulted in downward curves of ATPase activity, which reflect the back-inhibition of the pump. ATPase activities for SPCA1a wild-type and mutants at high Ca^{2+} (C) or Mn^{2+} (D) concentrations also displayed downward ATPase activity curves. One representative result is shown for each isoform or mutant. The standard deviation for each point is shown as error bar.

Suppl. Fig. 3. At 0.5 mM ATP, SPCA1a presents a biphasic activation pattern in ATPase assays
Via an enzyme-coupled assay, we determined the Ca^{2+} dependent ATPase activity of SPCA1a in the presence of 0.5 mM ATP. SPCA1a presents a two-step activation pattern (N = 4).

Suppl. Fig. 4. Native Page of purified SERCA1a and SPCA2 incubated with various amount of Ca^{2+}
SERCA1a (left) purified from skeletal muscle of rabbit or SPCA2 (right) overexpressed and purified from yeast were incubated with EGTA, 3 µM or 3 mM of $CaCl_2$, and separated by Native PAGE. The protein bands were visualized via de-staining for SERCA1a, or via immunoblotting for SPCA2 (SC376917, 1:2000, Santa Cruz). The monomer bands were indicated by arrows.

Suppl. Fig. 5. Maximal activities of the SPCA1a WT and the D41A/E50A mutant
ATPase activities (A) and auto-phosphorylation activity (B) of the D41A/E50A (AA) mutant normalized to the maximal activity of the WT in presence of Ca^{2+} (N = 3-6). One-way ANOVA was performed followed by *post-hoc* Bonferroni test. ** $P < 0.01$.

Suppl. Fig. 6. The effect of reducing agent and urea on SPCA1a obtained from microsomes
A. N-terminal mCherry tagged SPCA1a was overexpressed in HEK-293 cells. The microsome fraction was either not treated, or treated with reducing agent purchased from ThermoFisher Scientific Novex kit, with 40 mM reducing agent DTT, or with 8 M urea, with or without boiling, as indicated on top of each lane. Samples are then subjected to SDS-PAGE followed by immunoblotting using an SPCA1 antibody (Frodo, homemade, 1:50,000). B. Immunoblotting of the C-terminal His-tagged SPCA1a purified from yeast and reconstituted in proteoliposomes. The SPCA1a proteoliposomes are either not treated or treated with reducing agent purchased from ThermoFisher Scientific Novex kit, with 20 mM reducing agent TCEP and boiling, or with 8 M urea. These samples are then subjected to SDS-PAGE followed by immunoblotting with an SPCA1a antibody (Frodo, homemade, 1:50,000).